MORPHOLOGY OF VERY SMALL IMPACT CRATERS AT THE CHANG'E-3/4/5 LANDING REGIONS.

Yueyang Li[1], Wenzhe Fa[1], and Bojun Jia[1], [1]Institute of Remote Sensing and Geographical Information System, School of Earth and Space Sciences, Peking University, Beijing 100871, China (liyueyang0419@stu.pku.edu.cn; wzfa@pku.edu.cn; bjjia@pku.edu.cn)

Introduction: The morphology of impact craters at decimeter to hectometer scales can help to understand regolith properties, lunar surface evolution, and impact cratering process in the strength regime [1]. Though the morphology of craters above kilometer scales is well investigated, the morphology of craters at decimeter to hectometer scales (very small craters) is rarely studied due to the lack of high-resolution topography data. China's Chang'E-3/4/5 (CE-3/4/5) lunar landing missions have acquired high-resolution optical images and topography data with spatial resolution up to 5 mm/pixel, which provide an unprecedented opportunity to accurately extract the morphology of very small craters. In this study, we investigated the morphology of very small craters at the CE-3/4/5 landing regions, which can be further used in a wide range of studies (e.g., regolith thickness estimation, laboratory impact experiments, and radar observations).

Study Regions, Topography Data, and Morphological Parameters: The CE-3/4/5 landing regions are chosen as the study regions for the morphological investigation of very small craters. The CE-3 landing site is in an Eratosthenian-aged geological unit in the northern Mare Imbrium, east of Sinus Iridum [2]. The CE-4 landing site is on the floor of Von Kármán crater, northeast of the South Pole-Aitken (SPA) basin on the Moon's farside [3]. The CE-5 landing site is in a young geological unit named P58 in the northeast of Oceanus Procellarum [4]. The regolith thicknesses of the three landing regions are estimated to be 8, 12, and 5 m, respectively [2, 5, 4].

The optical images and topography data at the CE-3/4/5 landing regions are used to extract the morphology of very small craters (Fig. 1). There are three, seven, and one Digital Terrain Models (DTMs) at the CE-3, 4, and 5 landing regions with coverage areas of 1.2 km², 2800 m², and 3.8 km², respectively. The DTMs at the CE-3 and 5 landing regions are generated from the optical images acquired by the descent cameras with spatial resolutions of 0.05–0.5 m/pixel. The seven CE-4 DTMs are produced from the panoramic camera images onboard the CE-4 rover with spatial resolutions of 1 cm/pixel and 5 mm/pixel. The elevation accuracies of these topography data are better than decimeter scales, which is enough to accurately extract the morphology of very small craters.

The general process for crater morphological parameter extraction includes crater digitization in Digital Orthophoto Map (DOM) and topographic profile extraction in DTM. Detrending process, axisymmetric deviation refinement [6], and manual adjustment are introduced to reduce the influence of the background terrain and rectify the crater center position. The depth (d), rim height (h_r), and inner wall slope (S) are chosen to characterize the crater morphology.

Results and Discussion: 3150 craters are identified in the CE-3/4/5 DOMs. Considering the elevation accuracy of each topography data, the depths and inner wall slopes of 387, 681, and 445 craters with diameter ranges of 0.8–181.6 m, 0.14–3.68 m, and 10–192 m are extracted at the CE-3, 4 and 5 landing regions, respectively. The rim heights of 26, 308, and 25 craters at the CE-3, 4, and 5 landing regions are included in the final statistics. Based on these samples, the relations between the morphological parameters and crater diameters are fitted as (Fig. 2):

$$d = 0.059D^{1.010} \quad (1a)$$

$$h_r = 0.014D^{1.138} \quad (1b)$$

$$S = 92.964\ (d/D) + 4.409 \quad (1c)$$

The average d/D ratios of the craters at the CE-3, 4, and 5 landing regions are 0.069, 0.058, 0.072, and the inner wall slopes are 9.9˚, 9.1˚, 13.0˚, respectively. The mean d/D ratio, h_r/D ratio, and inner wall slope of all the craters at the three landing regions are 0.065, 0.017, and 10.5˚, respectively, all of which are smaller than those of large craters at hectometer scales (0.12, 0.04, and 22˚ [7, 8]).

The observed crater morphology can be ascribed to the effect of low-strength target materials upon crater formation and the fast degradation rate. Different from large craters (>100 m in diameter) that can penetrate the lunar regolith layer, most craters in our study are formed in the lunar regolith layer and in the strength-dominated regime. Thus the low-strength regolith layer is the major factor affecting the initial morphology of very small craters. The crater morphology differences among the three landing regions suggest that the CE-4, CE-3, and CE-5 landing regions have the highest, intermediate, and lowest regolith strengths, respectively, whereas the regolith densities at these sites follow an opposing trend.

Degradation simulations are performed on five craters with similar diameters (~2 m) and decreasing d/D ratios (0.118, 0.101, 0.087, 0.066, 0.044) at the CE-4 landing site. Compared to the corresponding

crater morphological classes for large craters (A, AB, B, BC, and C [9]), the five meter-scale craters have lower relative depths and gentler inner wall slopes than those larger craters at kilometer scales. In the degradation simulation, as craters degrade, the craters have shallower depths, more subdued rims, gentler wall slopes, and smoother outlines, which is consistent with the crater morphological prominence in the CE-4 panoramic images. The results also show that the lifetime of a 2-meter-diameter crater is ~3.97 Myr, which means that despite a meter-scale crater may be young in age, the crater could be highly degraded.

Meter-scale flat-bottomed and concentric craters are found in the three landing regions (Fig. 3). 248 meter-scale craters 1–7.2 m in diameter are identified by their shapes and shadow patterns in optical images, of which 206 craters are normal bowl-shaped and 42 are flat-bottomed or concentric. Most flat-bottomed and concentric craters are isolated and scattered across the landing regions, and some of them appear to cluster around the rim of nearby decameter-scale craters. Because most meter-scale craters can not penetrate the regolith layer, the strength variation within the superficial regolith layer is the possible cause for the formation of the flat-bottomed and concentric geometries. The vertical stratification within the regolith layer and uneven distribution of regolith are two possible mechanisms for the formation of the isolated and clustered very small craters with flat-bottomed and concentric geometries.

Conclusions: The morphologies of 1513 decimeter- to hectometer-scale craters at the CE-3/4/5 landing regions are analyzed using the high-resolution optical images and topography data. Analyses show that the morphology of very small craters can be ascribed to the effect of low-strength regolith on the initial crater morphology and the fast degradation rate. Meter-scale flat-bottomed and concentric craters are found in high-resolution optical images, which are probably caused by strength variation within the regolith layer. All these results can provide essential information for regolith physical properties, lunar surface evolution, and impact cratering mechanism at the meter scale or below.

Acknowledgment: This work was supported by the National Natural Science Foundation of China (12173004).

References: [1] Melosh H. J. (1989) *Impact Cratering: A Geologic Process,* Oxford Univ. Pr. [2] Fa W. et al. (2015) *GRL, 42(23),* 10179–10187. [3] Guo D. et al. (2021) *Icarus, 359,* 114327. [4] Jia B. et al. (2022) *EPSL, 596,* 117791. [5] Li C. et al. (2021) *Nature, 600,* 54–58. [6] Kokhanov A. A. et al. (2015) *Sol. Syst. Res., 49(5),* 295–302. [7] Stopar J. D. et al. (2017) *Icarus, 298,* 34–48. [8] Mahanti P. et al. (2018) *Icarus, 299,* 475–501. [9] Basilevsky A. T. (1976) *LPSC, 7,* 1914–1935.

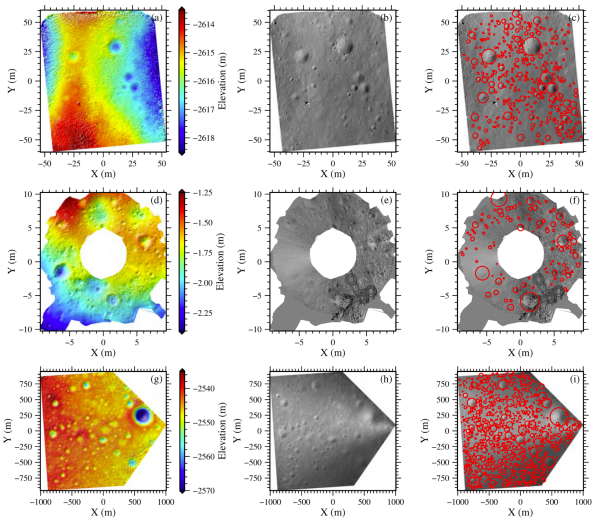

Figure 1. Topography data and the counted craters at the CE-3 (top), CE-4 (middle), and CE-5 (bottom) landing regions: (left) color-shaded maps of the DTMs, (middle) the DOMs, and (right) the counted craters.

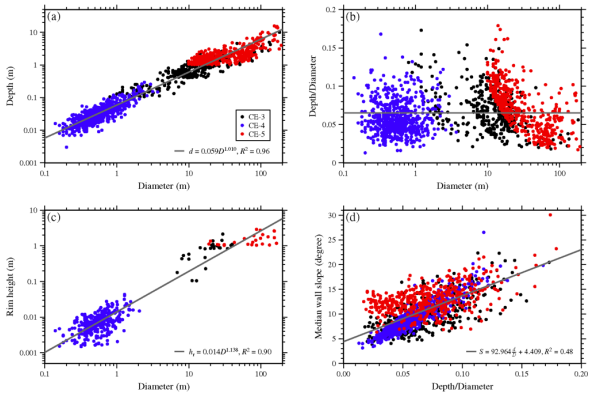

Figure 2. (a) Depth, (b) depth/diameter ratio, and (c) rim height as a function of diameter. (d) Inner wall slope as a function of depth/diameter ratio.

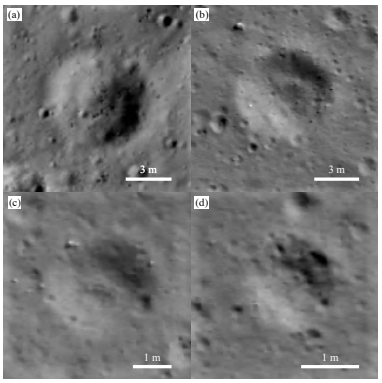

Figure 3. Meter-scale concentric (top) and flat-bottomed (bottom) craters at the CE-3/4/5 landing regions.